Preservation of organic traces of life under Martian conditions: Influence of the nature of the smectite in presence

I. Criouet, S. Bernard, E. Balan, F. Baron, A. Buch, F. Skouri-Panet, M. Guillaumet, L. Delbes, L. Remusat, J.-C. Viennet

Icarus 443 (2026) 116789

Contents lists available at ScienceDirect

Icarus

journal homepage: www.elsevier.com/locate/icarus

Research Paper

Preservation of organic traces of life under Martian conditions: Influence of the nature of the smectite in presence

I. Criouet [a], S. Bernard [a,*], E. Balan [a], F. Baron [b], A. Buch [c], F. Skouri-Panet [a], M. Guillaumet [a], L. Delbes [a], L. Remusat [a], J.-C. Viennet [a]

[a] Muséum National d'Histoire Naturelle, Sorbonne Université, UMR CNRS 7590, Institut de minéralogie, de physique des matériaux et de cosmochimie, Paris, France
[b] Université de Poitiers, CNRS, Institut de Chimie des Milieux et Matériaux de Poitiers (IC2MP) UMR, 7285 Poitiers, France
[c] Laboratoire Génie des Procédés et Matériaux, CentraleSupélec, Gif-sur-Yvette, France

ARTICLE INFO

Keywords:
Biosignatures
Mars
Fossilization
Clays
Smectites
Organics
Laboratory experiments

ABSTRACT

Clay-rich Martian rocks are considered promising targets in the search for fossilized remains of ancient Martian life. However, the actual influence of the clay mineral compositions in preserving microbial biosignatures remains poorly understood. Here, we explore the biopreservation potential of three pure smectites typically found on Mars and containing Al in their tetrahedral sheets (i.e. a Mg-rich, a Fe-rich and a Al-rich smectite), relying on experiments run using *E. coli* as a biological analog to simulate hydrothermal alteration scenarios relevant to Mars. The results show that Mg-rich smectites (saponite) are more effective at preserving biomolecules from thermal degradation than Fe-rich and Al-rich smectites (nontronite and beidellite). Plus, in contrast to saponite, neither nontronite nor beidellite appears to significantly trap (and thus preserve) organic compounds within their interlayer spaces. Overall, the present study highlights that both the chemistry and the abundance of organic material in ancient Martian clay-rich rocks will depend on the compositional nature of smectites initially present.

1. Introduction

NASA's Perseverance rover is currently collecting samples from Mars with the long-term goal of returning them to Earth for detailed analyses – including the search for past life (Farley et al., 2020). Ancient sedimentary rocks enriched in clay minerals such as smectites are particularly promising due to the high capacity of smectites to adsorb and preserve organic molecules (Hedges and Keil, 1995; Fairén et al., 2017), conferring smectites a high biopreservation potential (Ehlmann et al., 2008; Summons et al., 2008, 2011; McMahon et al., 2018; Bosak et al., 2021). However, the (sub)surface of Mars could not be ideal for the preservation of organic biosignatures. In fact, besides possible oxidation and radiation damages (Lasne et al., 2016; Fox et al., 2019; Megevand et al., 2021; Bernard et al., 2025), a major concern is the potential degradation of organic compounds caused by episodic fluid circulation (Viennet et al., 2019; Criouet et al., 2023a).

According to orbital and in-situ exploration, the majority of ancient Martian sedimentary rocks contain clay minerals (Ehlmann et al., 2008, 2011; Ehlmann and Edwards, 2014; Carter et al., 2013, 2015) and are intruded by veins (Schwenzer et al., 2016; Kronyak et al., 2019; Achilles et al., 2020; Bristow et al., 2021; Gasda et al., 2022; Farley et al., 2022; Clavé et al., 2023; Beck et al., 2025), which attests to the episodic circulation of fluids at variable temperatures since their deposition. In fact, the impact-induced melting of the excess ice locked in the Martian subsurface (Boynton, 2002; Bramson et al., 2015; Dundas et al., 2018; Piqueux et al., 2019) may have mobilized hot liquid water across vast distances (Rathbun and Squyres, 2002; Segura, 2002; Barnhart et al., 2010; Ivanov and Pierazzo, 2011; Osinski et al., 2013). Interactions with hot water have likely modified any organic compounds fossilized/trapped within the Martian rocks (McCollom et al., 2001; Lewan and Roy, 2011; Foustoukos and Stern, 2012), making it difficult to determine their origin. As a result, the exact nature of organic compounds that will be found in Martian rocks may differ significantly from current expectations.

In line with a number of experimental studies having investigated the possible influence of mineral phases on the thermal behavior of biogenic organic molecules (Montgomery et al., 2019; Royle et al., 2021a, 2021b, 2022), Tan et al. (2021) conducted artificial maturation experiments

* Corresponding author.
E-mail address: sbernard@mnhn.fr (S. Bernard).

https://doi.org/10.1016/j.icarus.2025.116789
Received 15 March 2025; Received in revised form 4 August 2025; Accepted 20 August 2025
Available online 21 August 2025

and showed that clay minerals mitigate the destructive influence of oxidizing minerals such as jarosite or goethite during hydrous pyrolysis by providing nondeleterious adsorption sites. Yet, they did not explore further the biopreservation potential of clay minerals. Noteworthy, the influence of the presence of octahedrally substituted smectites such as montmorillonites (montmorillonties are dioctahedral Al-rich smectites with a permanent charge in the octahedral layers) on the thermal evolution of organic compounds has been well documented (Yuan et al., 2013; Bu et al., 2017; Dalai et al., 2017; Du et al., 2021; Cai et al., 2022). Yet, most ancient Martian rocks contain tetrahedrally substituted, trioctahedral (saponite) or dioctahedral (nontronite and beidellite) smectites (Ehlmann et al., 2008; Bishop et al., 2011; Vaniman et al., 2014; Michalski et al., 2015). These smectites have a permanent charge in the tetrahedral layers and may host different cations in their octahedral sites (Mg for saponites, Fe for nontronites and Al for beidellites). This has its importance, since the compositional nature of smectites has been shown to control organic reactions, as demonstrated under simulated asteroidal conditions (Vinogradoff et al., 2020a, 2020b). So far, studies exploring the biopreservation potential of Martian smectites have relied on either nontronite (Gil-Lozano et al., 2020) or saponite (Viennet et al., 2019; Criouet et al., 2023a), but never both, making it difficult to discuss the actual biopreservation potential of different smectites under Martian conditions.

Recently, inspired by authors having explored the effect of diagenesis under terrestrial conditions (Oehler and Schopf, 1971; Li et al., 2014; Miot et al., 2017; Picard et al., 2015; Alleon et al., 2016; Igisu et al., 2018), Criouet et al. (2023a) used cultures of a model microorganism as starting materials for laboratory experiments (*E. coli* cells). These experiments were designed to mimic interactions with hot water in the presence of saponite (i.e. a Mg-rich trioctahedral smectite) under Martian conditions (i.e. a pure CO_2 atmosphere). Relying on experiments conducted at different temperatures for different durations, this study showed that the thermal degradation of microbial cells is delayed in the presence of saponite, with saponite selectively trapping nitrogen-rich organic compounds in its interlayer spaces. Altogether, this study demonstrated that some signals may persist in Martian rocks rich in saponite despite interactions with hot water. These results hold great promises for the future study of returned samples. Yet, results may differ with different smectites, such as nontronite or beidellite (i.e. tetrahedrally substituted dioctahedral smectites), which are widespread in Noachian terrains (i.e. terrains older than 3.7 Ga) (Ehlmann et al., 2008; Bishop et al., 2011; Vaniman et al., 2014; Michalski et al., 2015; Bristow et al., 2018).

For the present study, experiments were designed to interrogate the ability of different clay minerals to preserve biological materials during episodes of exposure to hot water. Mixtures of *E. coli* cells and smectites (either saponite, nontronite or beidellite) were exposed to water at 150 °C for 10 days, in closed systems, under a pure CO_2 atmosphere. Experiments were run at 150 °C to simulate hydrothermal alteration scenarios relevant to Mars. Most ancient Martian rocks have likely experienced such temperature at some point during their long history as a result of episodes of fluid circulation most often triggered by impacts (Rathbun and Squyres, 2002; Barnhart et al., 2010). Experiments were run for 10 days as most organic reactions occur within such a timeframe in such systems (Alleon et al., 2016, 2017; Criouet et al., 2023a) and under CO_2 to mimic a Martian atmosphere as atmospheric composition can influence organic reaction pathways (Schiffbauer et al., 2012; Viennet et al., 2020). Obviously, it should be kept in mind that the experiments conducted for the present study do not perfectly recreate the events that took place on Mars.

The solid residues of these experiments were recovered at the end to be characterized using the different techniques which are used on Mars and/or which are likely to be used to characterize the samples that will be brought back from Mars. In addition to elemental analyses, we used X-ray diffraction (XRD), Fourier-transform infrared (FTIR) spectroscopy and X-ray absorption near edge structure (XANES) spectroscopy to document the chemistry of the organic compounds and the nature and crystallinity of the smectites composing the residues. Additional XRD data were collected under vacuum on oriented preparations to investigate the possible storage of organic compounds within the interlayer spaces of the clay minerals composing the solid residues. Altogether, the results presented below demonstrate that both the abundance and preservation state of organics in ancient Martian clay-rich rocks are likely controlled by the chemistry and structure of the original smectite minerals.

2. Materials and methods

2.1. Starting materials

These experiments were designed to test the preservation potential of smectites, not microbial survivability. Thus, *Escherichia coli* was selected rather than extremophilic microorganisms to serve as a well-characterized model organism used broadly in microbial degradation studies (Li et al., 2014; Adamczyk and Reed, 2017; Moon et al., 2021; Dannenmann et al., 2023). Details on cultures of *E. coli* cells can be found in Criouet et al. (2023a). Briefly, a suspension of 10 mL of pre-cultured *E. coli* cells (C41 ccya B strain) was added to 1L of LB Lennox broth medium (20 g/L) (Sigma-Aldrich) that contained kanamycin (30 µg.mL-1) to inhibit the growth of other microbial strains. After being left to proliferate overnight, the cells were collected by centrifugation at 5000 rpm for 30 min, washed with distilled water before being dried at 50 °C overnight.

The tetrahedrally Al-substituted smectites selected for the present study (i.e. a saponite (Mg), a nontronite (Fe) and a beidellite (Al)) have previously been found on Mars (Ehlmann et al., 2008; Bishop et al., 2011; Vaniman et al., 2014; Michalski et al., 2015; Bristow et al., 2018). Details on the syntheses of saponite, nontronite and beidellite can be found in Criouet et al. (2023b). Briefly, diluted solutions of Na_2SiO_3 $5H_2O$ (Sigma Aldrich, >95 %), $AlCl_3$ $6H_2O$ (Sigma Aldrich, 99 %), $FeCl_3$ $6H_2O$ (Sigma Aldrich, >99 %) or $MgCl_2$ $6H_2O$ (Sigma Aldrich, >99 %) were mixed to produce gels stoichiometrically identical to either a saponite of composition $Na_{0.4}$ $(Si_{3.6}$ $Al_{0.4})$ Mg_3 O_{10} $(OH)_2$, a nontronite of composition $Na_{0.4}$ $(Si_{3.6}$ $Al_{0.4})$ Fe_2 O_{10} $(OH)_2$, or a beidellite of composition $Na_{0.4}$ $(Si_{3.6}$ $Al_{0.4})$ Al_2 O_{10} $(OH)_2$. Gels were then rinsed and filtered with milliQ water (18.2 MΩ-cm) to remove salts. The gel of nontronite was immersed in a pH 12.5 solution within a PTFE-lined Parr 4748 reactor for crystallization at 150 °C for 2.5 days (4.75 bars), the gel of beidellite into a solution at pH 12 for 9 days at 230 °C (~28 bars), and the gel of saponite into milliQ water for 10 days at 230 °C. The produced smectites were rinsed and filtered again with milliQ water before being dried at 50 °C overnight.

2.2. Experimental protocol

For the present study, 100 mg of pure smectite (either saponite, nontronite or beidellite) were mixed with 42 mg of dried *E. coli* cells (i.e. leading to a TOC (total organic carbon) of the mixture of 12.20 wt% as confirmed by measurements – Table 1) in 1 mL of pure water (milliQ - 18.2 MΩ-cm). Mixtures were loaded into Ti-reactors sealed in a dedicated glove box under an anoxic, pure CO_2 atmosphere before being exposed to 150 °C for 10 days in a dedicated oven. No salts were added in the system, but the water was in equilibrium with the smectites used for the experiments. Duplicate experiments were run to ensure reproducibility. Control experiments were also run, either without *E. coli* cells or without smectites, to assess background clay reactivity and organic stability under the conditions of the experiments (note that the three smectites used for the experiments do not undergo major structural modifications under the experimental conditions – cf. below).

At the end of the experiments, the water-soluble fractions were extracted from the solid residues by rinsing and centrifuging until the supernatant remained visually clear. Only the solid residues were

Table 1
EA-irIRMS results.

	$\%_{wt}$ C	$\%_{wt}$ N	N/C	δ^{13}C (‰)
E. coli cells	46.66	13.60	0.25	−24.74
Room Temperature	± 0.23	± 0.05		± 0.11
E. coli + H_2O + CO_2	70.27	6.51	0.08	−27.90
at 150 °C for 10 days	± 0.35	± 0.03		± 0.12
E. coli + Saponite, Nontronite or Beidellite	12.20	3.50	0.25	−24.96
Room Temperature	± 0.06	± 0.03		± 0.13
E. coli + Saponite + H_2O + CO_2	5.87	1.99	0.29	−24.65
at 150 °C for 10 days	± 0.03	± 0.01		± 0.11
E. coli + Nontronite + H_2O + CO_2	5.22	2.25	0.37	−25.03
at 150 °C for 10 days	± 0.03	± 0.01		± 0.11
E. coli + Beidellite + H_2O + CO_2	3.18	1.79	0.48	−25.68
at 150 °C for 10 days	± 0.02	± 0.01		± 0.11

analyzed after being dried at 50 °C overnight and ground by hand in an agate mortar for characterization. Residues of experiments conducted in the presence of smectites with *E. coli* cells were also dried on glass slides, at room temperature, to obtain oriented preparations for XRD.

Note that experiments were run at 150 °C to simulate hydrothermal alteration scenarios relevant to Mars. Most ancient Martian rocks have likely experienced such temperature at some point during their long history as a result of episodes of fluid circulation most often triggered by impacts (Rathbun and Squyres, 2002; Barnhart et al., 2010). Experiments were run for 10 days as most organic reactions occur within such a timeframe in such systems (Alleon et al., 2016, 2017) and under CO_2 to mimic a Martian atmosphere as atmospheric composition can influence organic reaction pathways (Schiffbauer et al., 2012; Viennet et al., 2020). In any case, these experiments were not aimed at perfectly mimicking the events that took place on Mars, but rather at interrogating the ability of different clay minerals to preserve biological materials during episodes of exposure to hot water.

2.3. Characterization techniques

2.3.1. Elemental analysis coupled to isotope ratio mass spectrometry (EA-IRMS)

Total organic carbon (TOC), total nitrogen (TN) contents, and carbon isotopic composition (δ^{13}C vs VPDB) were measured using a Flash 2000 Thermo CHNSO elemental analyzer coupled to a Thermo Fisher DeltaV Advantage IRMS (MNHN SSMIM, Paris). A mass of 1.2 mg of each residue was loaded in Sn-capsules and combusted under oxygen/helium flux at 1020 °C. The N_2 and CO_2 released by combustion were separated by a chromatography column and quantified using a thermal conductivity detector. The calibration was performed with 5 alanine standards (0.3 mg), and 10 other alanine standards (0.3 mg) were used to verify instrument performance.

2.3.2. Fourier-transform infrared spectroscopy (FTIR)

Mid-infrared (MIR) spectra were obtained from grounded samples measured using a Nicolet 6700 FTIR spectrometer (IMPMC, Paris) fitted with a KBr beamsplitter and a DTGS KBr detector. Spectra were recorded in the 400–4000 cm^{-1} range with a 4 cm^{-1} resolution, by averaging 150 scans obtained in attenuated total reflection mode (ATR) using a Specac Quest ATR device fitted with a diamond internal reflection element. The ATR mode allowed non-destructive analyses to be conducted on samples having experienced only minimal preparation.

2.3.3. X-ray diffraction (XRD)

The XRD data were collected at room temperature with a step size of 0.033°2θ over the 3–75°2θ Co k$\alpha_{1,2}$ angular range and a counting time of 300 ms per step using an X'Pert Pro instrument from PANalytical, equipped with a cobalt source (Co kα 40 mA) and operating at IMPMC (Paris, France). Oriented preparations from the residues of experiments conducted in the presence of saponite, nontronite and beidellite with *E. coli* cells were measured using the same instrument. XRD patterns were recorded at room temperature with a step size of 0.033°2θ over the 3–12°2θ Co k$\alpha_{1,2}$ angular range and a counting time of 300 ms per step. Measurements were performed at both atmospheric pressure and under vacuum (3.10^{-4} atm) to test for interlayer spacing changes indicative of organic intercalation using an Anton Parr HTK 1200 oven coupled to an EDWARDS RV3 pump.

2.3.4. Scanning transmission X-ray microscopy (STXM) - X-ray absorption near edge structure (XANES) spectroscopy

Five samples were selected for these analyzes: (1) untreated *E. coli*, (2) heat-treated *E. coli* control, (3) heat-treated *E. coli* + saponite, (4) heat-treated *E. coli* + nontronite, (5) heat-treated *E. coli* + beidellite. Samples were first prepared by cryo-ultramicrotome sections (100 nm thick) using a Leica cryo-ultramicrotome at UMET (Lille, France), following the protocol of Jacquemot et al. (2019) allowing to obtain ultrathin samples while preserving fine-scale organic-clay associations. Powders of experimental residues were mixed with 0.1 ml of milliQ water. A drop of the mixture was frozen in liquid nitrogen at −120 °C and cut using a diamond-knife. Then, the ultrathin slices of residues were deposited on holey carbon film TEM grids. Scanning transmission X-ray microscopy (STXM) analyses were performed at high spatial resolution (25 nm) on these ultrathin slices to document the carbon speciation of degraded cells in the presence of the three smectites using the HERMES STXM beamline at the synchrotron SOLEIL (Saint-Aubin, France) (Belkhou et al., 2015; Swaraj et al., 2017). Energy calibration was done using the well-resolved 3p Rydberg peak of gaseous CO_2 at 294.96 eV for the C K-edge. X-ray absorption near edge structure (XANES) hypercube data (stacks) were collected at energy increments of 0.1 eV over the carbon (270–350 eV) absorption range with a dwell time of ≤1 ms per pixel to prevent irradiation damage (Wang et al., 2009). Stack alignments and extraction of XANES spectra were done using the free and open source Python code Hyperspy. Using the method described in Le Guillou et al. (2018) to normalize the spectra to the carbon quantity, background was subtracted using a power law before integrating the spectra up to the mean ionization energy of carbon atoms (e.g., up to 291.5 eV at the C K edge).

3. Results and discussion

3.1. Stability of Smectites

Results of experiments run without *E. coli* cells demonstrate that the three investigated smectites remain structurally stable under the experimental conditions: neither their XRD patterns nor their FTIR spectra show significant changes after 10 days at 150 °C (Figs. 1 & 2). This is also the case for experiments run with *E. coli* cells (Figs. 1 & 2), except for an irrationality in the 00l reflection series of each of the smectites ($\ell \times d_{00\ell} \neq d_{001}$), as well as other noticeable changes in the XRD pattern and FTIR spectrum of the nontronite. This irrationality likely indicates the coexistence of different hydration states or layer types, possibly due to structural heterogeneities affecting the layer charge distribution and/or location, as reported by Ferrage et al. (2010). Plus, peak broadening (i.e. the 001 and 004 reflections) may suggest a reduction in coherent domain size, consistent with partial structural disorder or degradation (Grauby et al., 1994). Note that the nontronite composing the residue obtained with *E. coli* cells shows new diffraction peaks at 4.41 and 2.43 Å (Fig. 1), as shown by the clays observed on Mars at Gale crater and interpreted as glauconitic clays (Losa-Adams et al., 2021). These new peaks could correspond to the (−111) and (−132) reflections of a higher-charge nontronite with a better layer stacking and/or a slightly different distribution of octahedral Fe compared the starting nontronite. Consistently, an increase in layer charge could also be deduced from the slight shift of the FTIR νFe_2^{3+}-OH vibration to lower wavenumbers (Fig. 2) as it may indicate the partial reduction of some octahedral Fe(III), increasing the layer charge (Stucki et al., 2002). Last, two additional diffraction peaks can be observed at

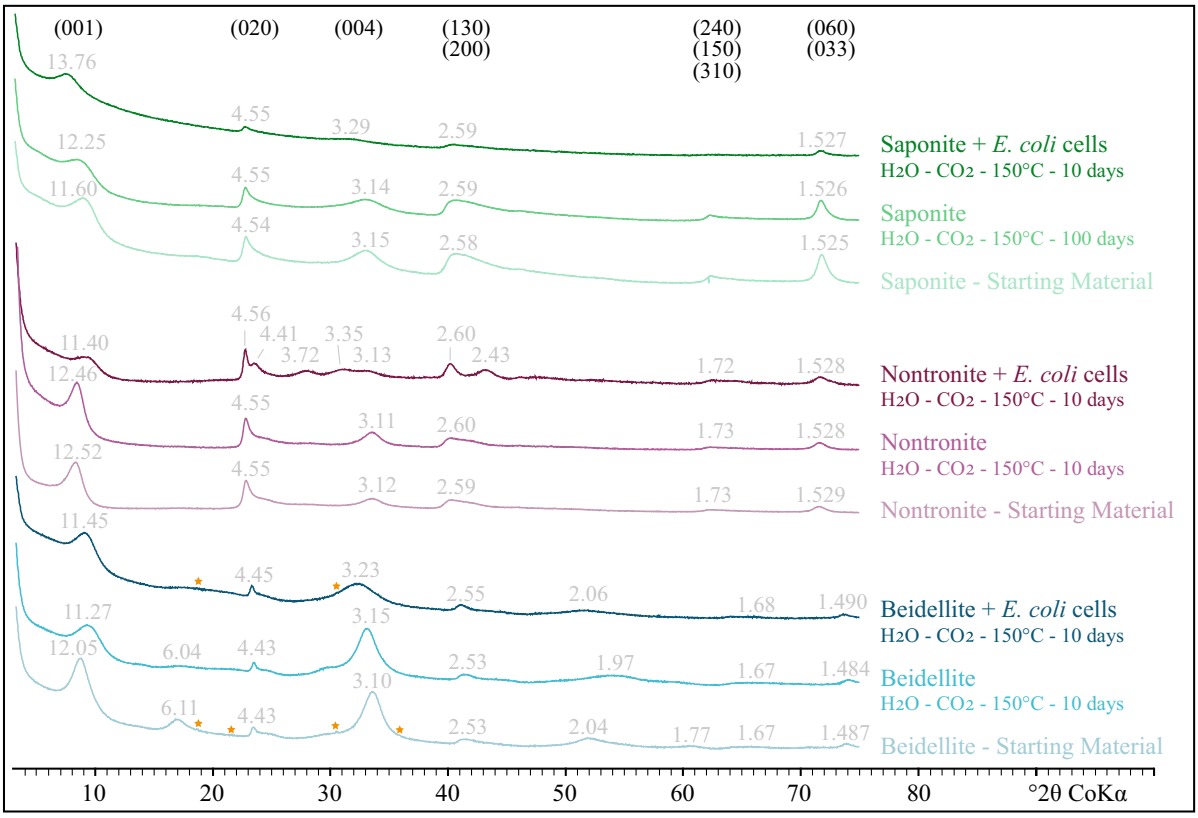

Fig. 1. XRD patterns of powdered experimental residues and starting materials collected at 1 atm. Orange stars highlight the presence of traces of Analcime.

3.72 and 3.35 Å (Fig. 1) and may correspond to 003 and 004 reflections of a nontronite having trapped organic compounds or ammonium ions in some interlayer spaces (Aranda and Ruiz-Hitzky, 1999).

3.2. Thermal degradation of *E. coli* cells

When placed at 150 °C for 10 days in the absence of smectite, *E. coli* cells experience chemical transformations, as indicated by the high TOC, the low N/C, and the more negative $\delta^{13}C$ values of the residue compared to the values of the starting material (Table 1). Consistently, the relative intensities of the FTIR absorption bands of the residue corresponding to organics bonds (i.e. amides A νN-H at 3278 cm^{-1}, amides B νN-H at 3060 cm^{-1}, $\nu_{as}CH_3$, $\nu_{as}CH_2$, ν_sCH_3 and ν_sCH_2 at 2959, 2921, 2873 and 2852 cm^{-1}, amides I νC=O at 1645 and 1631 cm^{-1}, amides II δN-H and νC-N at 1557 cm^{-1}, νC=C or νC=N 1515 cm^{-1}, δC-H at 1465 cm^{-1} and 1452 cm^{-1}, carboxylic νC=O or δC-H at 1402 and 1385 cm^{-1}, and amide III or phosphate groups at 1226 cm^{-1} - Li et al., 2014; Criouet et al., 2023a) are different from those of the starting material (Fig.2). In particular, the ratio between the FTIR bands in the 1300–600 cm^{-1} range (attributed to C—N, C—O and P═O bonds) and the FTIR bands at 1515 and 1695 cm^{-1} (attributed to C═C and C═O bonds) is lower than that of pristine *E. coli* cells (Fig. 2 - Li et al., 2014), indicating a loss of oxygen- and nitrogen-rich functional groups relative to unsaturated carbon structures. Similar conclusions can be drawn from XANES data, the residue obtained without smectite exhibiting a lower concentration in amide and hydroxyl functional groups (peaks at 288.2 and 289.5 eV - Le Guillou et al., 2018) and a higher concentration in aromatic functional groups (peaks at 285 and 285.5 eV) than pristine *E. coli* cells (Fig. 3). Such evolution (i.e. progressive aromatization and defunctionalization) is typical of biogenic organic compounds having experienced thermal maturation (Bernard and Horsfield, 2014; Bernard et al., 2015; Alleon et al., 2017).

3.3. Influence of smectites

The presence of smectite has had a noticeable influence on the chemistry of organic materials. This is not that surprising, since smectites are known to play a key role in the thermal maturation of organic compounds (Johns, 1979; Horsfield and Douglas, 1980; Goldstein, 1983; Nikalje et al., 2000), via possible interactions with Lewis and Brønsted sites (i.e. at the edges or within the interlayer volume) (Yuan et al., 2013; Bu et al., 2017; Du et al., 2021; Cai et al., 2022).

Here, although less than the starting materials, the residues of the experiments run with smectites still contain some organic material (as indicated by TOC values - Table 1). These organic materials exhibit $\delta^{13}C$ values not significantly different from the values displayed by pristine *E. coli* cells, but the N/C values are higher (Table 1). Plus, except for the residue of experiments run with saponite (which FTIR spectrum resembles that of the starting mixture), the organic materials in the residues obtained with nontronite or beidellite show FTIR absorption bands with different relative ratios (Fig. 2). Also, a new and intense absorption band at about near 1420 cm^{-1}, attributed to NH_4^+ vibrations (Pironon et al., 2003; Petit et al., 2006; Gautier et al., 2010), can be observed in the FTIR spectra of the residues produced in the presence of nontronite or beidellite (Fig. 2). The presence of NH_4^+ ions within the interlayer spaces of smectites (cf below) may explain the high N/C values of the residues.

In line with FTIR data, XANES data show that the organic material of the residue obtained with saponite is very similar to that pristine *E. coli* cells, with a main feature attributed to amide functional groups (peak et 288.2 eV - Alleon et al., 2017). The presence of saponite thus seems to enhance the preservation of original biochemical functionality. In contrast, the XANES spectra of the residues obtained with nontronite or beidellite are dominated by benzoquinones or unsaturated carbonyls and carboxylic moieties (peaks at 284.8 and 288.6 eV - Cooney and Urquhart, 2004; Le Guillou et al., 2018), even though these were low abundant to absent in the starting materials (Fig. 3). This shows that the

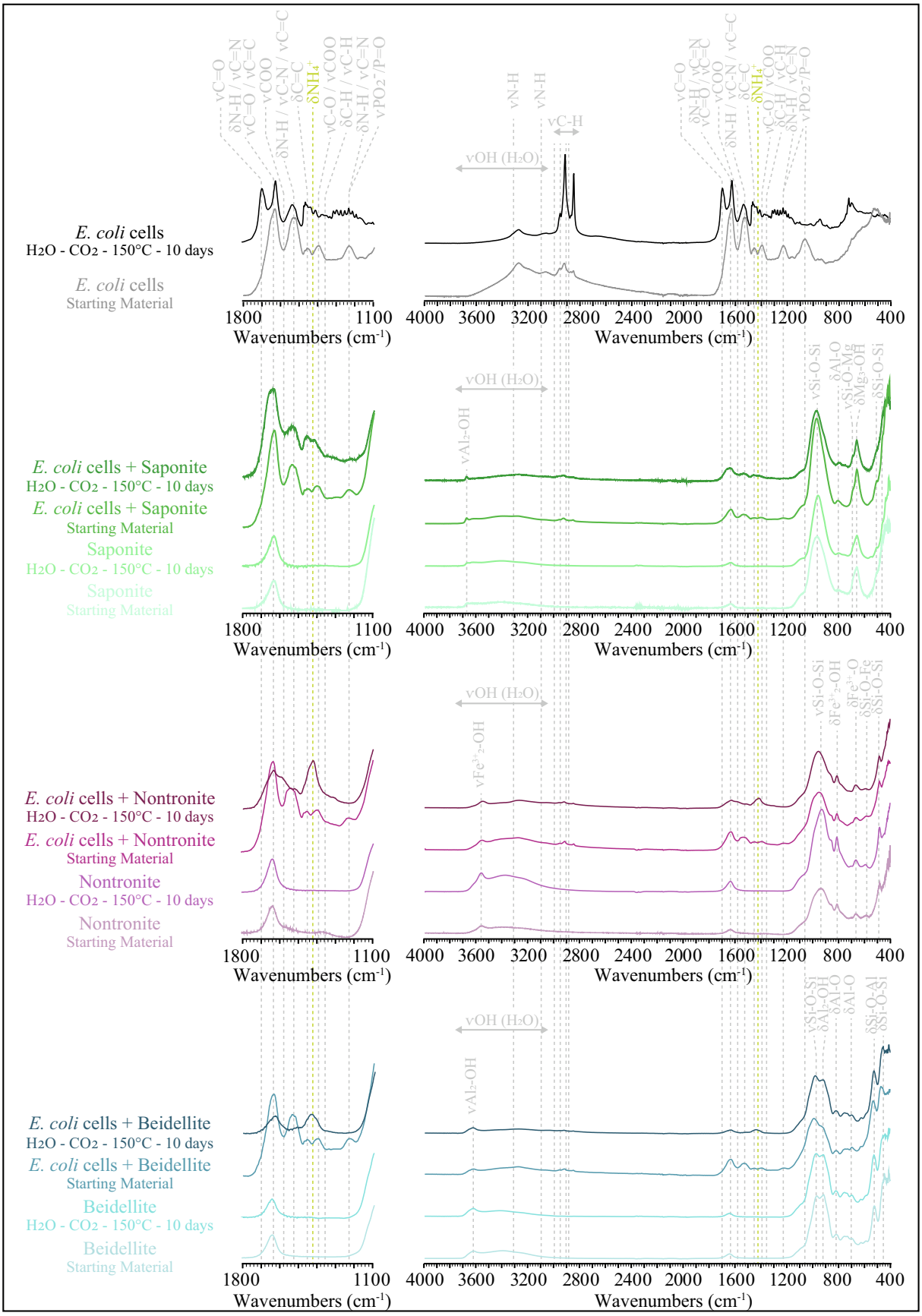

Fig. 2. FTIR spectra of experimental residues and starting materials.

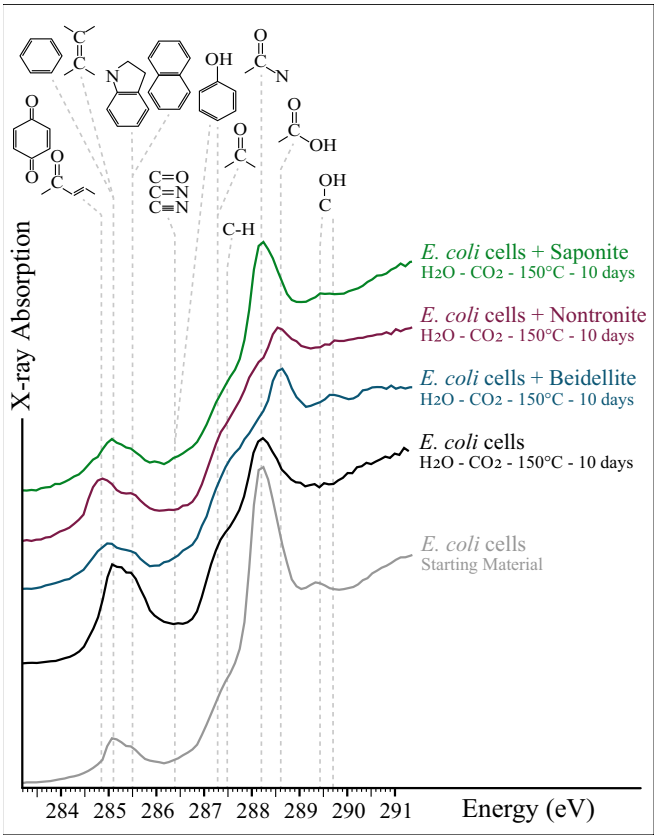

Fig. 3. C-XANES spectra of experimental residues and starting material.

starting organic material underwent deamination during the experiments run with nontronite and beidellite, possibly producing the NH_4^+ ions that ended up stored within the interlayer spaces of these smectites (cf below). The presence of nontronite or beidellite thus leads to more extensive deamination and oxidation of biogenic organic material compared to saponite. All in all, the experiments reported here demonstrate that the chemical nature of the organic material possibly trapped within Martian clay-rich sediments having experienced episodes of exposure to fluids will depend on the compositional nature of smectites initially present.

3.4. Focus on dioctahedral smectites

Although nontronite and beidellite are both dioctahedral smectites, one can observe chemical differences between the residues obtained with these smectites. First, the N/C value of the residue obtained with beidellite is significantly higher (Table 1), suggesting that either the residual organic material contains more N or that beidellite has stored more NH_4^+ within its interlayer spaces. According to XANES data, the organic material in the residue obtained with beidellite possibly contain imine and/or nitrile functional groups, as shown by the shoulder centered at 286.4 (Fig. 3 - Le Guillou et al., 2018). However, this organic material does not seem to contain amide groups, as indicated by both FTIR and XANES data, in contrast to the one obtained with nontronite, which XANES spectrum displays a shoulder at 288.2 eV attributed to amide groups and which FTIR spectrum exhibits features at 1630 and 3280 cm^{-1} attributed to amide νNH and νC=O (Fig. 2&3 - Li et al., 2014; Alleon et al., 2017; Le Guillou et al., 2018; Criouet et al., 2023a). The starting organic material thus seems to have experienced more deamination in the presence of beidellite than in the presence of nontronite, as indicated by N/C values and FTIR and XANES spectra. Plus, although slightly richer in (benzo)quinones, the organic material in the residue obtained with nontronite seems to contain less carboxylic and hydroxyl groups, as shown by the less intense features at 288.6 and 289.7 eV (Fig. 3 - Le Guillou et al., 2018). Although possibly related to pH (which could unfortunately not be measured in the present study given the very low amounts of fluids), these chemical differences may also be due to oxidation reactions having occurred during the experiments. If so, Fe(III) could have been the ultimate electron acceptors in the presence of nontronite, while it requires invoking the electron deficiency of Al in the presence of beidellite (Helmboldt et al., 2007; Hicks et al., 2018). In other words, Fe(III) in nontronite may have acted as an internal oxidant, whereas in Al-rich beidellite, oxidative degradation may have originated from electron-deficient structural sites. This result is noteworthy as nontronite has previously been reported to mitigate the UV-induced degradation of organic materials (dos Santos et al., 2016), suggesting that its biopreservation potential may strongly vary depending on the environmental conditions. In any case, in contrast to saponite, neither nontronite nor beidellite seems to be efficient in protecting biogenic organic compounds from thermal degradation and oxidation, their presence even acting as factors limiting the preservation of organic biosignatures during episodes of fluid circulation.

3.5. Storage of organic compounds

The use of XRD under vacuum helps identifying the possible presence of organic materials in the interlayer spaces of smectites. In fact, these spaces may not fully collapse under vacuum if organic carbon or ammonium ions are stored within (Criouet et al., 2023a; Viennet et al., 2023). Here, XRD data collected under vacuum confirm the presence of organic materials within the interlayer spaces of the saponite composing the residues (Fig. 4). Yet, the interlayer spacings of the nontronite and beidellite composing the residues appear to retain predominantly NH_4^+

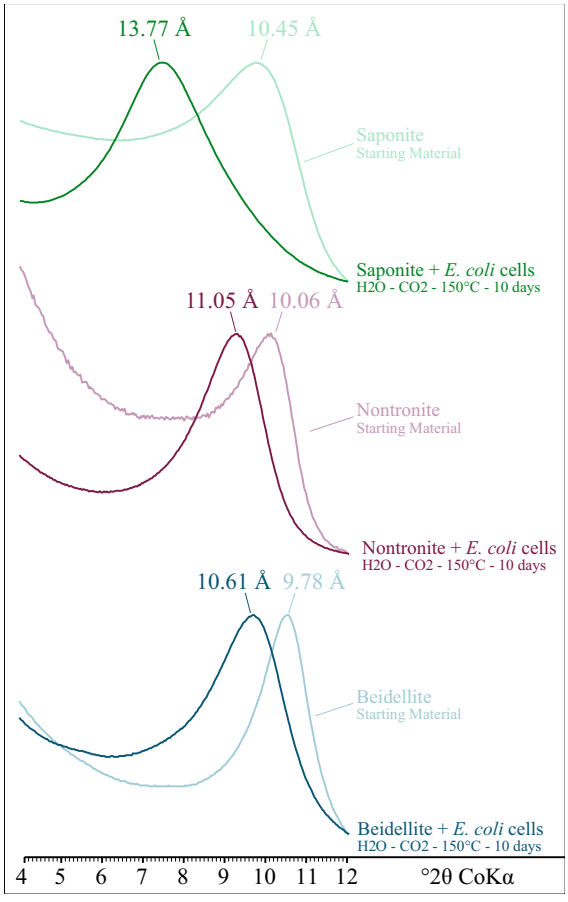

Fig. 4. XRD patterns of experimental residues and starting materials collected under vacuum on oriented preparations.

(likely released by the deamination of the proteins of *E. coli* cells), their layer to layer distances under vacuum being identical to that of NH_4^+-saturated smectites (Fig. 4 - Morida et al., 2023), explaining the high N/C values of the residues and the absorption band attributed to NH_4^+ vibrations in the FTIR spectra (cf above). Thus, in contrast to saponite, neither nontronite nor beidellite seems to particularly store organic materials within their interlayer spaces. This again may be related to pH, organic-smectite interactions being strongly pH-dependent (Jaber et al., 2018; Gil-Lozano et al., 2020). For instance, the adsorption of a protein is optimal at pH close to its isoelectric point (Jaber et al., 2018). Consistently, Gil-Lozano et al. (2020) reported that the intercalation of glycine in the interlayer spaces of nontronites via cationic exchange occurs less at low pH than at high pH, demonstrating that the pH of the fluid to which smectites have been exposed will affect their biopreservation potential under Mars surface conditions.

3.6. Future directions

The experiments reported here demonstrate the influence of the presence of smectites on the preservation of organic compounds, highlighting that all smectitic clay minerals do not share the same potential for biopreservation under (simulated) Martian conditions. However, it remains challenging to extrapolate experimental results to natural settings. The experiments reported here have been designed to interrogate the ability of different clay minerals to preserve biological materials during episodes of exposure to hot water, rather than to mimic the complexity of natural settings, which cannot be done in the laboratory (Bernard et al., 2015; Alleon et al., 2017; Criouet et al., 2023a). Still, one may wonder how different results may be in open systems. This can be tested by designing fluid-flow experiments to be compared to experiments conducted in closed systems. Similarly, the nature/salinity of the fluid (or fluids) may influence organic reactions as well as interactions with smectites. Thus, instead of a fluid in equilibrium with the smectites in presence (as is the case here), future experiments could be conducted with fluids out of equilibrium, such as silica-rich, carbonate-rich or sulfate-rich fluids, given that Martian sediments have interacted with a huge diversity of fluids (Kronyak et al., 2019; Achilles et al., 2020; Bristow et al., 2021; Gasda et al., 2022; Farley et al., 2022; Clavé et al., 2023; Beck et al., 2025). Last, the organic content of Martian rocks has likely suffered from electromagnetic (UV and γ) and particle (protons, neutrons and high Z atoms) radiation and/or from the presence of strong oxidants (Lasne et al., 2016; Fox et al., 2019; Megevand et al., 2021; Bernard et al., 2025), which effects were not investigated in the present study. Nevertheless, although the precise influence of a number of parameters and processes have yet to be quantified, there is little question that laboratory experiments, even relying on simplified systems, will nourish Mars astrobiological research aiming at eventually providing evidence for traces of extraterrestrial life.

4. Conclusion

Beyond their potential involvement in the origin of life (Cairns-Smith, 1966; Kloprogge and Hartman, 2022), clay minerals also contribute to the preservation of biosignatures. In fact, the present study shows that both both the nature and abundance of organic material possibly trapped within Martian clay-rich sediments having experienced episodes of exposure to fluids will depend on the mineralogical nature of smectites initially present. In fact, the present work highlights that even subtle chemical variations in the hosting clays may be critical for the long-term preservation of organic traces of life under Martian conditions. In other words, all smectitic clay minerals do not share the same potential for biopreservation. This insight extends beyond Mars: investigating solely the chemical nature of organic compounds in a rock may not be sufficient when exploring for potential biosignatures, whether this rock comes from Earth, Mars or beyond, including aqueously altered carbon-rich small bodies such as Europa, Enceladus or Ceres (Nordheim et al., 2018; Postberg et al., 2018; Marchi et al., 2019; Muñoz-Iglesias et al., 2021), a number of small bodies having been shown to contain ammonia and/or ammonium-rich smectites (King et al., 1992; Berg et al., 2016; Viennet et al., 2023; Glavin et al., 2025). Thus, in addition to the geological history, precisely documenting the nature of the organo-mineral assemblage in ancient rocks should be seen as necessary to discuss the origin (biogenic or abiotic) of the organic materials in presence.

CRediT authorship contribution statement

I. Criouet: Writing – original draft, Visualization, Methodology, Investigation, Formal analysis, Data curation, Conceptualization. **S. Bernard:** Writing – original draft, Visualization, Validation, Supervision, Project administration, Methodology, Investigation, Funding acquisition, Formal analysis, Data curation, Conceptualization. **E. Balan:** Methodology, Investigation, Formal analysis, Data curation. **F. Baron:** Methodology, Investigation, Formal analysis, Data curation. **A. Buch:** Methodology, Investigation, Formal analysis, Data curation. **F. Skouri-Panet:** Methodology, Investigation, Formal analysis, Data curation. **M. Guillaumet:** Methodology, Investigation, Formal analysis, Data curation. **L. Delbes:** Methodology, Investigation, Formal analysis, Data curation. **L. Remusat:** Validation, Supervision, Resources, Project administration, Funding acquisition. **J.-C. Viennet:** Writing – original draft, Visualization, Validation, Supervision, Methodology, Investigation, Formal analysis, Data curation, Conceptualization.

Declaration of competing interest

The authors declare that they have no known competing financial interests or personal relationships that could have appeared to influence the work reported in this paper.

Acknowledgments

The authors wish to acknowledge the spectroscopic and X-ray diffraction facilities of IMPMC. The HERMES beamline (SOLEIL) is supported by the CNRS, the CEA, the Region Ile de France, the Conseil Départemental de l'Essonne and the Region Centre. This work was made possible thanks to financial support from the ATM program at MNHN (Project BioMars - PI: S. Bernard), from the Institut des Matériaux of Sorbonne Université (IMat) (Project Ageing on Mars - PI: S. Bernard) and from the European Research Council (ERC Consolidator Grant No. 819587: HYDROMA - PI: L. Remusat). The authors declare that they have no known competing financial interests or personal relationships that could have appeared to influence the work reported in this article.

Data availability

All data used in the present study are publicly available at Zenodo with a Creative Commons Attribution 4.0 license (Criouet, 2025 – doi: https://doi.org/10.5281/zenodo.14634605).

References

Achilles, C.N., Rampe, E.B., Downs, R.T., Bristow, T.F., Ming, D.W., Morris, R.V., Vaniman, D.T., Blake, D.F., Yen, A.S., McAdam, A.C., Sutter, B., Fedo, C.M., Gwizd, S., Thompson, L.M., Gellert, R., Morrison, S.M., Treiman, A.H., Crisp, J.A., Gabriel, T.S.J., Chipera, S.J., Hazen, R.M., Craig, P.I., Thorpe, M.T., Des Marais, D.J., Grotzinger, J.P., Tu, V.M., Castle, N., Downs, G.W., Peretyazhko, T.S., Walroth, R.C., Sarrazin, P., Morookian, J.M., 2020. Evidence for multiple diagenetic episodes in ancient fluvial-lacustrine sedimentary rocks in Gale Crater, Mars. JGR Planets 125, e2019JE006295. https://doi.org/10.1029/2019JE006295.

Adamczyk, P.A., Reed, J.L., 2017. Escherichia coli as a model organism for systems metabolic engineering. Curr. Opin. Syst. Biol. 6, 80–88. https://doi.org/10.1016/j.coisb.2017.11.001.

Alleon, J., Bernard, S., Le Guillou, C., Daval, D., Skouri-Panet, F., Pont, S., Delbes, L., Robert, F., 2016. Early entombment within silica minimizes the molecular

degradation of microorganisms during advanced diagenesis. Chem. Geol. 437, 98–108. https://doi.org/10.1016/j.chemgeo.2016.05.034.
Alleon, J., Bernard, S., Le Guillou, C., Daval, D., Skouri-Panet, F., Kuga, M., Robert, F., 2017. Organic molecular heterogeneities can withstand diagenesis. Sci. Rep. 7. https://doi.org/10.1038/s41598-017-01612-8.
Aranda, P., Ruiz-Hitzky, E., 1999. Poly(ethylene oxide)/NH4+-smectite nanocomposites. Appl. Clay Sci. 15, 119–135. https://doi.org/10.1016/S0169-1317(99)00015-0.
Barnhart, C.J., Nimmo, F., Travis, B.J., 2010. Martian post-impact hydrothermal systems incorporating freezing. Icarus 208, 101–117. https://doi.org/10.1016/j.icarus.2010.01.013.
Beck, P., Beyssac, O., Dehouck, E., Bernard, S., Pineau, M., Mandon, L., Royer, C., Clavé, E., Schröder, S., Forni, O., Francis, R., Mangold, N., Bedford, C.C., Broz, A.P., Cloutis, E.A., Johnson, J.R., Poulet, F., Fouchet, T., Quantin-Nataf, C., Pilorget, C., Rapin, W., Meslin, P.-Y., Gabriel, T.S.J., Arana, G., Madariaga, J.M., Brown, A.J., Maurice, S., Clegg, S.M., Gasnault, O., Cousin, A., Wiens, R.C., 2025. From hydrated silica to quartz: potential hydrothermal precipitates found in Jezero crater, Mars. Earth Planet. Sci. Lett. 656, 119256. https://doi.org/10.1016/j.epsl.2025.119256.
Belkhou, R., Stanescu, S., Swaraj, S., Besson, A., Ledoux, M., Hajlaoui, M., Dalle, D., 2015. HERMES: a soft X-ray beamline dedicated to X-ray microscopy. J. Synchrotron Radiat. 22, 968–979. https://doi.org/10.1107/S1600577515007778.
Berg, B.L., Cloutis, E.A., Beck, P., Vernazza, P., Bishop, J.L., Takir, D., Reddy, V., Applin, D., Mann, P., 2016. Reflectance spectroscopy (0.35–8 μm) of ammonium-bearing minerals and qualitative comparison to Ceres-like asteroids. Icarus 265, 218–237. https://doi.org/10.1016/j.icarus.2015.10.028.
Bernard, S., Beyssac, O., Manrique, J.A., Lopez Reyes, G., Ollila, A., Le Mouélic, S., Beck, P., Pilleri, P., Forni, O., Julve-González, S., Veneranda, M., Reyes Rodriguez, I., Madariaga, J.M., Aramenda, J., Castro, K., Clavé, E., Royer, C., Fornaro, T., Bousquet, B., Sharma, S.K., Johnson, J.R., Cloutis, E., Gabriel, T.S.J., Meslin, P.Y., Gasnault, O., Cousin, A., Wiens, R.C., Maurice, S., 2025. Ageing of organic materials at the surface of Mars: A Raman study aboard Perseverance. Geochem. Persp. Let. 34, 25–30. https://doi.org/10.7185/geochemlet.2509.
Bernard, S., Horsfield, B., 2014. Thermal maturation of gas shale systems. Annu. Rev. Earth Planet. Sci. 42, 635–651. https://doi.org/10.1146/annurev-earth-060313-054850.
Bernard, S., Benzerara, K., Beyssac, O., Balan, E., Brown Jr., G.E., 2015. Evolution of the macromolecular structure of sporopollenin during thermal degradation. Heliyon 1, e00034. https://doi.org/10.1016/j.heliyon.2015.e00034.
Bishop, J.L., Gates, W.P., Makarewicz, H.D., McKeown, N.K., Hiroi, T., 2011. Reflectance spectroscopy of Beidellites and their importance for Mars. Clay Clay Miner. 59, 378–399. https://doi.org/10.1346/CCMN.2011.0590403.
Bosak, T., Moore, K.R., Gong, J., Grotzinger, J.P., 2021. Searching for biosignatures in sedimentary rocks from early earth and Mars. Nat Rev Earth Environ 2, 490–506. https://doi.org/10.1038/s43017-021-00169-5.
Boynton, W.V., 2002. Distribution of hydrogen in the near surface of Mars: evidence for subsurface ice deposits. Science 297, 81–85. https://doi.org/10.1126/science.1073722.
Bramson, A.M., Byrne, S., Putzig, N.E., Sutton, S., Plaut, J.J., Brothers, T.C., Holt, J.W., 2015. Widespread excess ice in Arcadia Planitia, Mars. Geophys. Res. Lett. 42, 6566–6574. https://doi.org/10.1002/2015GL064844.
Bristow, T.F., Rampe, E.B., Achilles, C.N., Blake, D.F., Chipera, S.J., Craig, P., Crisp, J.A., Des Marais, D.J., Downs, R.T., Gellert, R., 2018. Clay mineral diversity and abundance in sedimentary rocks of Gale crater, Mars. Sci. Adv. 4, eaar3330.
Bristow, T.F., Grotzinger, J.P., Rampe, E.B., Cuadros, J., Chipera, S.J., Downs, G.W., Fedo, C.M., Frydenvang, J., McAdam, A.C., Morris, R.V., Achilles, C.N., Blake, D.F., Castle, N., Craig, P., Des Marais, D.J., Downs, R.T., Hazen, R.M., Ming, D.W., Morrison, S.M., Thorpe, M.T., Treiman, A.H., Tu, V., Vaniman, D.T., Yen, A.S., Gellert, R., Mahaffy, P.R., Wiens, R.C., Bryk, A.B., Bennett, K.A., Fox, V.K., Millken, R.E., Fraeman, A.A., Vasavada, A.R., 2021. Brine-driven destruction of clay minerals in Gale crater, Mars. Science 373, 198–204. https://doi.org/10.1126/science.abg5449.
Bu, H., Yuan, P., Liu, H., Liu, D., Liu, J., He, H., Zhou, J., Song, H., Li, Z., 2017. Effects of complexation between organic matter (OM) and clay mineral on OM pyrolysis. Geochim. Cosmochim. Acta 212, 1–15. https://doi.org/10.1016/j.gca.2017.04.045.
Cai, J., Du, J., Song, M., Lei, T., Wang, X., Li, Y., 2022. Control of clay mineral properties on hydrocarbon generation of organo-clay complexes: evidence from high-temperature pyrolysis experiments. Appl. Clay Sci. 216, 106368. https://doi.org/10.1016/j.clay.2021.106368.
Cairns-Smith, A.G., 1966. The origin of life and the nature of the primitive gene. J. Theor. Biol. 10, 53–88. https://doi.org/10.1016/0022-5193(66)90178-0.
Carter, J., Poulet, F., Bibring, J.-P., Mangold, N., Murchie, S., 2013. Hydrous minerals on Mars as seen by the CRISM and OMEGA imaging spectrometers: updated global view: HYDROUS MINERALS ON MARS: GLOBAL VIEW. J. Geophys. Res. Planets 118, 831–858. https://doi.org/10.1029/2012JE004145.
Carter, J., Loizeau, D., Mangold, N., Poulet, F., Bibring, J.-P., 2015. Widespread surface weathering on early Mars: a case for a warmer and wetter climate. Icarus 248, 373–382. https://doi.org/10.1016/j.icarus.2014.11.011.
Clavé, E., Benzerara, K., Meslin, P.-Y., Forni, O., Royer, C., Mandon, L., Beck, P., Quantin-Nataf, C., Beyssac, O., Cousin, A., Bousquet, B., Wiens, R.C., Maurice, S., Dehouck, E., Schröder, S., Gasnault, O., Mangold, N., Dromart, G., Bosak, T., Bernard, S., Udry, A., Anderson, R.B., Arana, G., Brown, A.J., Castro, K., Clegg, S.M., Cloutis, E., Fairén, A.G., Flannery, D.T., Gasda, P.J., Johnson, J.R., Lasue, J., Lopez-Reyes, G., Madariaga, J.M., Manrique, J.A., Le Mouélic, S., Núñez, J.I., Ollila, A.M., Pilleri, P., Pilorget, C., Pinet, P., Poulet, F., Veneranda, M., Wolf, Z.U., the SuperCam team, 2023. Carbonate detection with SuperCam in igneous rocks on the floor of Jezero Crater, Mars. JGR Planets 128, e2022JE007463. https://doi.org/10.1029/2022JE007463.
Cooney, R.R., Urquhart, S.G., 2004. Chemical trends in the near-edge X-ray absorption fine structure of Monosubstituted and Para-Bisubstituted benzenes. J. Phys. Chem. B 108, 18185–18191. https://doi.org/10.1021/jp046868j.
Criouet, I., Viennet, J.C., Baron, F., Balan, E., Buch, A., Delbes, L., Guillaumet, M., Remusat, L., Bernard, S., 2023b. Influence of pH on the hydrothermal synthesis of Al-substituted Smectites (Saponite, Beidellite, and Nontronite). Clay Clay Miner. 71, 539–558. https://doi.org/10.1007/s42860-023-00255-3.
Criouet, Isis, Viennet, J.-C., Balan, E., Baron, F., Buch, A., Skouri-Panet, F., Guillaumet, M., Delbes, L., Remusat, L., Bernard, S., 2023a. Experimental investigations of the preservation/degradation of microbial signatures in the presence of clay minerals under Martian subsurface conditions. Icarus 406, 115743. https://doi.org/10.1016/j.icarus.2023.115743.
Dalai, P., Pleyer, H.L., Strasdeit, H., Fox, S., 2017. The influence of mineral matrices on the thermal behavior of Glycine. Orig. Life Evol. Biosph. 47, 427–452. https://doi.org/10.1007/s11084-016-9523-0.
Dannenmann, M., Klenner, F., Bönigk, J., Pavlista, M., Napoleoni, M., Hillier, J., Khawaja, N., Olsson-Francis, K., Cable, M.L., Malaska, M.J., Abel, B., Postberg, F., 2023. Toward detecting biosignatures of DNA, lipids, and metabolic intermediates from Bacteria in ice grains emitted by Enceladus and Europa. Astrobiology 23, 60–75. https://doi.org/10.1089/ast.2022.0063.
Du, J., Cai, J., Lei, T., Li, Y., 2021. Diversified roles of mineral transformation in controlling hydrocarbon generation process, mechanism, and pattern. Geosci. Front. 12, 725–736. https://doi.org/10.1016/j.gsf.2020.08.009.
Dundas, C.M., Bramson, A.M., Ojha, L., Wray, J.J., Mellon, M.T., Byrne, S., McEwen, A. S., Putzig, N.E., Viola, D., Sutton, S., Clark, E., Holt, J.W., 2018. Exposed subsurface ice sheets in the Martian mid-latitudes. Science 359, 199–201. https://doi.org/10.1126/science.aao1619.
Ehlmann, B.L., Edwards, C.S., 2014. Mineralogy of the Martian surface. Annu. Rev. Earth Planet. Sci. 42, 291–315. https://doi.org/10.1146/annurev-earth-060313-055024.
Ehlmann, B.L., Mustard, J.F., Fassett, C.I., Schon, S.C., Head III, J.W., Des Marais, D.J., Grant, J.A., Murchie, S.L., 2008. Clay minerals in delta deposits and organic preservation potential on Mars. Nat. Geosci. 1, 355–358. https://doi.org/10.1038/ngeo207.
Ehlmann, B.L., Mustard, J.F., Murchie, S.L., Bibring, J.-P., Meunier, A., Fraeman, A.A., Langevin, Y., 2011. Subsurface water and clay mineral formation during the early history of Mars. Nature 479, 53–60. https://doi.org/10.1038/nature10582.
Fairén, A.G., Gil-Lozano, C., Uceda, E.R., Losa-Adams, E., Davila, A.F., Gago-Duport, L., 2017. Mineral paragenesis on Mars: the roles of reactive surface area and diffusion. JGR Planets 122, 1855–1879. https://doi.org/10.1002/2016JE005229.
Farley, K.A., Williford, K.H., Stack, K.M., Bhartia, R., Chen, A., De La Torre, M., Hand, K., Goreva, Y., Herd, C.D.K., Hueso, R., Liu, Y., Maki, J.N., Martinez, G., Moeller, R.C., Nelessen, A., Newman, C.E., Nunes, D., Ponce, A., Spanovich, N., Willis, P.A., Beegle, L.W., Bell, J.F., Brown, A.J., Hamran, S.-E., Hurowitz, J.A., Maurice, S., Paige, D.A., Rodriguez-Manfredi, J.A., Schulte, M., Wiens, R.C., 2020. Mars 2020 Mission overview. Space Sci. Rev. 216, 142. https://doi.org/10.1007/s11214-020-00762-y.
Farley, K.A., Stack, K.M., Shuster, D.L., Horgan, B.H.N., Hurowitz, J.A., Tarnas, J.D., Simon, J.I., Sun, V.Z., Scheller, E.L., Moore, K.R., McLennan, S.M., Vasconcelos, P. M., Wiens, R.C., Treiman, A.H., Mayhew, L.E., Beyssac, O., Kizovski, T.V., Tosca, N. J., Williford, K.H., Crumpler, L.S., Beegle, L.W., Bell, J.F., Ehlmann, B.L., Liu, Y., Maki, J.N., Schmidt, M.E., Allwood, A.C., Amundsen, H.E.F., Bhartia, R., Bosak, T., Brown, A.J., Clark, B.C., Cousin, A., Forni, O., Gabriel, T.S.J., Goreva, Y., Gupta, S., Hamran, S.-E., Herd, C.D.K., Hickman-Lewis, K., Johnson, J.R., Kah, L.C., Kelemen, P.B., Kinch, K.B., Mandon, L., Mangold, N., Quantin-Nataf, C., Rice, M.S., Russell, P.S., Sharma, S., Siljeström, S., Steele, A., Sullivan, R., Wadhwa, M., Weiss, B.P., Williams, A.J., Wogsland, B.V., Willis, P.A., Acosta-Maeda, T.A., Beck, P., Benzerara, K., Bernard, S., Burton, A.S., Cardarelli, E.L., Chide, B., Clavé, E., Cloutis, E.A., Cohen, B.A., Czaja, A.D., Debaille, V., Dehouck, E., Fairén, A.G., Flannery, D.T., Fleron, S.Z., Fouchet, T., Frydenvang, J., Garczynski, B.J., Gibbons, E.F., Hausrath, E.M., Hayes, A.G., Henneke, J., Jørgensen, J.L., Kelly, E.M., Lasue, J., Le Mouélic, S., Madariaga, J.M., Maurice, S., Merusi, M., Meslin, P.-Y., Milkovich, S.M., Million, C.C., Moeller, R.C., Núñez, J.I., Ollila, A.M., Paar, G., Paige, D.A., Pedersen, D.A.K., Pilleri, P., Pilorget, C., Pinet, P.C., Rice, J.W., Royer, C., Sautter, V., Schulte, M., Sephton, M.A., Sharma, S.K., Sholes, S.F., Spanovich, N., St. Clair, M., Tate, C.D., Uckert, K., VanBommel, S.J., Yanchilina, A. G., Zorzano, M.-P., 2022. Aqueously altered igneous rocks sampled on the floor of Jezero crater, Mars. Science 377, eabo2196. https://doi.org/10.1126/science.abo2196.
Ferrage, E., Lanson, B., Michot, L.J., Robert, J.-L., 2010. Hydration properties and interlayer Organization of Water and Ions in synthetic Na-Smectite with tetrahedral layer charge. Part 1. Results from X-ray diffraction profile modeling. J. Phys. Chem. C 114, 4515–4526. https://doi.org/10.1021/jp909860p.
Foustoukos, D.I., Stern, J.C., 2012. Oxidation pathways for formic acid under low temperature hydrothermal conditions: implications for the chemical and isotopic evolution of organics on Mars. Geochim. Cosmochim. Acta 76, 14–28. https://doi.org/10.1016/j.gca.2011.10.016.
Fox, A.C., Eigenbrode, J.L., Freeman, K.H., 2019. Radiolysis of macromolecular organic material in Mars-relevant mineral matrices. J. Geophys. Res. Planets 124, 3257–3266. https://doi.org/10.1029/2019JE006072.
Gasda, P.J., Comellas, J., Essunfeld, A., Das, D., Bryk, A.B., Dehouck, E., Schwenzer, S.P., Crossey, L., Herkenhoff, K., Johnson, J.R., Newsom, H., Lanza, N.L., Rapin, W., Goetz, W., Meslin, P., Bridges, J.C., Anderson, R., David, G., Turner, S.M.R., Thorpe, M.T., Kah, L., Frydenvang, J., Kronyak, R., Caravaca, G., Ollila, A., Le Mouélic, S., Nellessen, M., Hoffman, M., Fey, D., Cousin, A., Wiens, R.C., Clegg, S.M., Maurice, S., Gasnault, O., Delapp, D., Reyes-Newell, A., 2022. Overview of the morphology and chemistry of diagenetic features in the clay-rich Glen Torridon unit

of Gale crater, Mars. JGR Planets 127, e2021JE007097. https://doi.org/10.1029/2021JE007097.
Gautier, M., Muller, F., Le Forestier, L., Beny, J.-M., Guegan, R., 2010. NH4-smectite: characterization, hydration properties and hydro mechanical behaviour. Appl. Clay Sci. 49, 247–254. https://doi.org/10.1016/j.clay.2010.05.013.
Gil-Lozano, C., Fairén, A.G., Muñoz-Iglesias, V., Fernández-Sampedro, M., Prieto-Ballesteros, O., Gago-Duport, L., Losa-Adams, E., Carrizo, D., Bishop, J.L., Fornaro, T., Mateo-Martí, E., 2020. Constraining the preservation of organic compounds in Mars analog nontronites after exposure to acid and alkaline fluids. Sci. Rep. 10, 15097. https://doi.org/10.1038/s41598-020-71657-9.
Glavin, D.P., Dworkin, J.P., Alexander, C.M.O., Aponte, J.C., Baczynski, A.A., Barnes, J. J., Bechtel, H.A., Berger, E.L., Burton, A.S., Caselli, P., Chung, A.H., Clemett, S.J., Cody, G.D., Dominguez, G., Elsila, J.E., Farnsworth, K.K., Foustoukos, D.I., Freeman, K.H., Furukawa, Y., Gainsforth, Z., Graham, H.V., Grassi, T., Giuliano, B. M., Hamilton, V.E., Haenecour, P., Heck, P.R., Hofmann, A.E., House, C.H., Huang, Y., Kaplan, H.H., Keller, L.P., Kim, B., Koga, T., Liss, M., McLain, H.L., Marcus, M.A., Matney, M., McCoy, T.J., McIntosh, O.M., Mojarro, A., Naraoka, H., Nguyen, A.N., Nuevo, M., Nuth, J.A., Oba, Y., Parker, E.T., Peretyazhko, T.S., Sandford, S.A., Santos, E., Schmitt-Kopplin, P., Seguin, F., Simkus, D.N., Shahid, A., Takano, Y., Thomas-Keprta, K.L., Tripathi, H., Weiss, G., Zheng, Y., Lunning, N.G., Righter, K., Connolly, H.C., Lauretta, D.S., 2025. Abundant ammonia and nitrogen-rich soluble organic matter in samples from asteroid (101955) Bennu. Nat Astron 9, 199–210. https://doi.org/10.1038/s41550-024-02472-9.
Goldstein, T.P., 1983. Geocatalytic reactions in formation and maturation of petroleum. Bulletin 67. https://doi.org/10.1306/03B5ACD7-16D1-11D7-8645000102C1865D.
Grauby, O., Petit, S., Decarreau, A., Baronnet, A., 1994. The nontronite-saponite series: an experimental approach. Eur. J. Mineral. 99–112.
Hedges, J.I., Keil, R.G., 1995. Sedimentary organic matter preservation: an assessment and speculative synthesis. Mar. Chem. 49, 81–115. https://doi.org/10.1016/0304-4203(95)00008-F.
Helmboldt, O., Keith Hudson, L., Misra, C., Wefers, K., Heck, W., Stark, H., Danner, M., Rösch, N., 2007. Aluminum compounds, inorganic. In: Wiley-VCH (Ed.), Ullmann's Encyclopedia of Industrial Chemistry. Wiley, pp. 1–17. https://doi.org/10.1002/14356007.a01_527.pub2.
Hicks, J., Vasko, P., Goicoechea, J.M., Aldridge, S., 2018. Synthesis, structure and reaction chemistry of a nucleophilic aluminyl anion. Nature 557, 92–95. https://doi.org/10.1038/s41586-018-0037-y.
Horsfield, B., Douglas, A.G., 1980. The influence of minerals on the pyrolysis of kerogens. Geochim. Cosmochim. Acta 44, 1119–1131. https://doi.org/10.1016/0016-7037(80)90066-6.
Igisu, M., Yokoyama, T., Ueno, Y., Nakashima, S., Shimojima, M., Ohta, H., Maruyama, S., 2018. Changes of aliphatic C-H bonds in cyanobacteria during experimental thermal maturation in the presence or absence of silica as evaluated by FTIR microspectroscopy. Geobiology 16, 412–428. https://doi.org/10.1111/gbi.12294.
Ivanov, B.A., Pierazzo, E., 2011. Impact cratering in H2O-bearing targets on Mars: thermal field under craters as starting conditions for hydrothermal activity: thermal field under Martian impact craters. Meteorit. Planet. Sci. 46, 601–619. https://doi.org/10.1111/j.1945-5100.2011.01177.x.
Jaber, M., Lambert, J.-F., Balme, S., 2018. Protein adsorption on clay minerals. In: Developments in Clay Science. Elsevier, pp. 255–288. https://doi.org/10.1016/B978-0-08-102432-4.00008-1.
Jacquemot, P., Viennet, J.-C., Bernard, S., Le Guillou, C., Rigaud, B., Delbes, L., Georgelin, T., Jaber, M., 2019. The degradation of organic compounds impacts the crystallization of clay minerals and vice versa. Sci. Rep. 9. https://doi.org/10.1038/s41598-019-56756-6.
Johns, W.D., 1979. Clay mineral catalysis and petroleum generation. Annu. Rev. Earth Planet. Sci. 7, 183–198. https://doi.org/10.1146/annurev.ea.07.050179.001151.
King, T.V.V., Clark, R.N., Calvin, W.M., Sherman, D.M., Brown, R.H., 1992. Evidence for ammonium-bearing minerals on Ceres. Science 255, 1551–1553. https://doi.org/10.1126/science.255.5051.1551.
Kloprogge, J.T. (Theo), Hartman, H., 2022. Clays and the origin of life: the experiments. Life 12, 259. https://doi.org/10.3390/life12020259.
Kronyak, R.E., Kah, L.C., Edgett, K.S., VanBommel, S.J., Thompson, L.M., Wiens, R.C., Sun, V.Z., Nachon, M., 2019. Mineral-filled fractures as indicators of multigenerational fluid flow in the Pahrump Hills member of the Murray formation, Gale crater, Mars. Earth Space Sci. 6, 238–265. https://doi.org/10.1029/2018EA000482.
Lasne, J., Noblet, A., Szopa, C., Navarro-González, R., Cabane, M., Poch, O., Stalport, F., François, P., Atreya, S.K., Coll, P., 2016. Oxidants at the surface of Mars: a review in light of recent exploration results. Astrobiology 16, 977–996. https://doi.org/10.1089/ast.2016.1502.
Le Guillou, C., Bernard, S., De la Pena, F., Le Brech, Y., 2018. XANES-based quantification of carbon functional group concentrations. Anal. Chem. 90, 8379–8386. https://doi.org/10.1021/acs.analchem.8b00689.
Lewan, M.D., Roy, S., 2011. Role of water in hydrocarbon generation from type-I kerogen in mahogany oil shale of the Green River formation. Org. Geochem. 42, 31–41. https://doi.org/10.1016/j.orggeochem.2010.10.004.
Li, J., Bernard, S., Benzerara, K., Beyssac, O., Allard, T., Cosmidis, J., Moussou, J., 2014. Impact of biomineralization on the preservation of microorganisms during fossilization: an experimental perspective. Earth Planet. Sci. Lett. 400, 113–122. https://doi.org/10.1016/j.epsl.2014.05.031.
Losa-Adams, E., Gil-Lozano, C., Fairén, A.G., Bishop, J.L., Rampe, E.B., Gago-Duport, L., 2021. Long-lasting habitable periods in Gale crater constrained by glauconitic clays. Nat Astron 5, 936–942. https://doi.org/10.1038/s41550-021-01397-x.
Marchi, S., Raponi, A., Prettyman, T.H., De Sanctis, M.C., Castillo-Rogez, J., Raymond, C. A., Ammannito, E., Bowling, T., Ciarniello, M., Kaplan, H., Palomba, E., Russell, C.T., Vinogradoff, V., Yamashita, N., 2019. An aqueously altered carbon-rich Ceres. Nat. Astron. 3, 140–145. https://doi.org/10.1038/s41550-018-0656-0.
McCollom, T.M., Seewald, J.S., Simoneit, B.R.T., 2001. Reactivity of monocyclic aromatic compounds under hydrothermal conditions. Geochim. Cosmochim. Acta 65, 455–468. https://doi.org/10.1016/S0016-7037(00)00533-0.
McMahon, S., Bosak, T., Grotzinger, J.P., Milliken, R.E., Summons, R.E., Daye, M., Newman, S.A., Fraeman, A., Williford, K.H., Briggs, D.E.G., 2018. A field guide to finding fossils on Mars. J. Geophys. Res. Planets 123, 1012–1040. https://doi.org/10.1029/2017JE005478.
Megevand, V., Viennet, J.C., Balan, E., Gauthier, M., Rosier, P., Morand, M., Garino, Y., Guillaumet, M., Pont, S., Beyssac, O., Bernard, S., 2021. Impact of UV radiation on the Raman signal of Cystine: implications for the detection of S-rich organics on Mars. Astrobiology 21, 566–574. https://doi.org/10.1089/ast.2020.2340.
Michalski, J.R., Cuadros, J., Bishop, J.L., Darby Dyar, M., Dekov, V., Fiore, S., 2015. Constraints on the crystal-chemistry of Fe/Mg-rich smectitic clays on Mars and links to global alteration trends. Earth Planet. Sci. Lett. 427, 215–225. https://doi.org/10.1016/j.epsl.2015.06.020.
Miot, J., Bernard, S., Bourreau, M., Guyot, F., Kish, A., 2017. Experimental maturation of Archaea encrusted by Fe-phosphates. Sci. Rep. 7. https://doi.org/10.1038/s41598-017-17111-9.
Montgomery, W., Jaramillo, E.A., Royle, S.H., Kounaves, S.P., Schulze-Makuch, D., Sephton, M.A., 2019. Effects of oxygen-containing salts on the detection of organic biomarkers on Mars and in terrestrial analog soils. Astrobiology 19, 711–721. https://doi.org/10.1089/ast.2018.1888.
Moon, A., Meshram, V., Khan, D., Pise, A., Mirza, A., Ukey, H., Dandekar, K., Meghakewalramani, Khatri P., Meshram, S., Mishra, S., 2021. *Escherichia coli*:A Model Organism in Life Science Research. International J. Innovat. Res. Sci. Eng. Technol. 10. https://doi.org/10.15680/IJIRSET.2021.1007075|.
Morida, K., Fukushi, K., Sakuma, H., Tamura, K., 2023. Systematic comparison of the hydration and dehydration of Na+−, K+-, and NH4+-saturated montmorillonite, nontronite, hectorite, saponite, and Fe-saponite by in situ X-ray diffraction measurements. Appl. Clay Sci. 237, 106898. https://doi.org/10.1016/j.clay.2023.106898.
Muñoz-Iglesias, V., Fernández-Sampedro, M., Gil-Lozano, C., Bonales L., J., Ercilla Herrero, O., Valles González, M.P., Mateo-Martí, E., Prieto-Ballesteros, O., 2021. Characterization of NH4-montmorillonite under conditions relevant to Ceres. Appl. Clay Sci. 209, 106137. https://doi.org/10.1016/j.clay.2021.106137.
Nikalje, M.D., Phukan, P., Sudalai, A., 2000. Recent advances in clay-catalyzed organic transformations. Org. Prep. Proced. Int. 32, 1–40. https://doi.org/10.1080/00304940009356743.
Nordheim, T.A., Hand, K.P., Paranicas, C., 2018. Preservation of potential biosignatures in the shallow subsurface of Europa. Nat. Astron. 2, 673–679. https://doi.org/10.1038/s41550-018-0499-8.
Oehler, J.H., Schopf, J.W., 1971. Artificial microfossils: experimental studies of Permineralization of blue-green algae in silica. Science 174, 1229–1231. https://doi.org/10.1126/science.174.4015.1229.
Osinski, G.R., Tornabene, L.L., Banerjee, N.R., Cockell, C.S., Flemming, R., Izawa, M.R. M., McCutcheon, J., Parnell, J., Preston, L.J., Pickersgill, A.E., Pontefract, A., Sapers, H.M., Southam, G., 2013. Impact-generated hydrothermal systems on earth and Mars. Icarus 224, 347–363. https://doi.org/10.1016/j.icarus.2012.08.030.
Petit, S., Righi, D., Madejová, J., 2006. Infrared spectroscopy of NH4+-bearing and saturated clay minerals: a review of the study of layer charge. Appl. Clay Sci. 34, 22–30. https://doi.org/10.1016/j.clay.2006.02.007.
Picard, A., Kappler, A., Schmid, G., Quaroni, L., Obst, M., 2015. Experimental diagenesis of organo-mineral structures formed by microaerophilic Fe(II)-oxidizing bacteria. Nat. Commun. 6, 6277. https://doi.org/10.1038/ncomms7277.
Piqueux, S., Buz, J., Edwards, C.S., Bandfield, J.L., Kleinböhl, A., Kass, D.M., Hayne, P.O., The MCS, THEMIS Teams, 2019. Widespread shallow water ice on Mars at high Latitudesand Midlatitudes. Geophys. Res. Lett. https://doi.org/10.1029/2019GL083947.
Pironon, J., Pelletier, M., De Donato, P., Mosser-Ruck, R., 2003. Characterization of smectite and illite by FTIR spectroscopy of interlayer NH_4^+ cations. Clay Miner. 38, 201–211. https://doi.org/10.1180/0009855033820089.
Postberg, F., Khawaja, N., Abel, B., Choblet, G., Glein, C.R., Gudipati, M.S., Henderson, B. L., Hsu, H.-W., Kempf, S., Klenner, F., Moragas-Klostermeyer, G., Magee, B., Nölle, L., Perry, M., Reviol, R., Schmidt, J., Srama, R., Stolz, F., Tobie, G., Trieloff, M., Waite, J.H., 2018. Macromolecular organic compounds from the depths of Enceladus. Nature 558, 564–568. https://doi.org/10.1038/s41586-018-0246-4.
Rathbun, J.A., Squyres, S.W., 2002. Hydrothermal systems associated with Martian impact craters. Icarus 157, 362–372. https://doi.org/10.1006/icar.2002.6838.
Royle, S.H., Tan, J.S.W., Watson, J.S., Sephton, M.A., 2021a. Pyrolysis of carboxylic acids in the presence of Iron oxides: implications for life detection on missions to Mars. Astrobiology 21, 673–691. https://doi.org/10.1089/ast.2020.2226.
Royle, S.H., Watson, J.S., Sephton, M.A., 2021b. Transformation of cyanobacterial biomolecules by Iron oxides during flash pyrolysis: implications for Mars life-detection missions. Astrobiology 21, 1363–1386. https://doi.org/10.1089/ast.2020.2428.
Royle, S.H., Salter, T.L., Watson, J.S., Sephton, M.A., 2022. Mineral matrix effects on pyrolysis products of kerogens infer difficulties in determining biological provenance of macromolecular organic matter at Mars. Astrobiology 22, 520–540. https://doi.org/10.1089/ast.2021.0074.
dos Santos, R., Patel, M., Cuadros, J., Martins, Z., 2016. Influence of mineralogy on the preservation of amino acids under simulated Mars conditions. Icarus 277, 342–353. https://doi.org/10.1016/j.icarus.2016.05.029.

Schiffbauer, J.D., Wallace, A.F., Hunter, J.L., Kowalewski, M., Bodnar, R.J., Xiao, S., 2012. Thermally-induced structural and chemical alteration of organic-walled microfossils: an experimental approach to understanding fossil preservation in metasediments: experimental thermal alteration of microfossils. Geobiology 10, 402–423. https://doi.org/10.1111/j.1472-4669.2012.00332.x.

Schwenzer, S.P., Bridges, J.C., Wiens, R.C., Conrad, P.G., Kelley, S.P., Leveille, R., Mangold, N., Martín-Torres, J., McAdam, A., Newsom, H., Zorzano, M.P., Rapin, W., Spray, J., Treiman, A.H., Westall, F., Fairén, A.G., Meslin, P.-Y., 2016. Fluids during diagenesis and sulfate vein formation in sediments at Gale crater, Mars. Meteorit. Planet. Sci. 51, 2175–2202. https://doi.org/10.1111/maps.12668.

Segura, T.L., 2002. Environmental effects of large impacts on Mars. Science 298, 1977–1980. https://doi.org/10.1126/science.1073586.

Stucki, J.W., Lee, K., Zhang, L., Larson, R.A., 2002. Effects of iron oxidation states on the surface and structural properties of smectites. Pure Appl. Chem. 74, 2145–2158. https://doi.org/10.1351/pac200274112145.

Summons, R.E., Albrecht, P., McDonald, G., Moldowan, J.M., 2008. Molecular Biosignatures. Space Sci. Rev. 135, 133–159. https://doi.org/10.1007/s11214-007-9256-5.

Summons, R.E., Amend, J.P., Bish, D., Buick, R., Cody, G.D., Des Marais, D.J., Dromart, G., Eigenbrode, J.L., Knoll, A.H., Sumner, D.Y., 2011. Preservation of Martian organic and environmental records: final report of the Mars biosignature working group. Astrobiology 11, 157–181. https://doi.org/10.1089/ast.2010.0506.

Swaraj, S., Belkhou, R., Stanescu, S., Rioult, M., Besson, A., Hitchcock, A.P., 2017. Performance of the HERMES beamline at the carbon K-edge. J. Phys. Conf. Ser. 849, 012046. https://doi.org/10.1088/1742-6596/849/1/012046.

Tan, J.S.W., Royle, S.H., Sephton, M.A., 2021. Artificial maturation of iron- and sulfur-rich Mars analogues: Implications for the diagenetic stability of biopolymers and their detection with pyrolysis–gas chromatography–mass spectrometry. Astrobiology 21, 199–218. https://doi.org/10.1089/ast.2019.2211.

Vaniman, D.T., Bish, D.L., Ming, D.W., Bristow, T.F., Morris, R.V., Blake, D.F., Chipera, S. J., Morrison, S.M., Treiman, A.H., Rampe, E.B., Rice, M., Achilles, C.N., Grotzinger, J.P., McLennan, S.M., Williams, J., Bell, J.F., Newsom, H.E., Downs, R.T., Maurice, S., Sarrazin, P., Yen, A.S., Morookian, J.M., Farmer, J.D., Stack, K., Milliken, R.E., Ehlmann, B.L., Sumner, D.Y., Berger, G., Crisp, J.A., Hurowitz, J.A., Anderson, R., Des Marais, D.J., Stolper, E.M., Edgett, K.S., Gupta, S., Spanovich, N., Science Team, M.S.L., Agard, C., Alves Verdasca, J.A., Anderson, Ryan, Archer, D., Armiens-Aparicio, C., Arvidson, R., Atlaskin, E., Atreya, S., Aubrey, A., Baker, B., Baker, M., Balic-Zunic, T., Baratoux, D., Baroukh, J., Barraclough, B., Bean, K., Beegle, L., Behar, A., Bender, S., Benna, M., Bentz, J., Berger, J., Berman, D., Blanco Avalos, J.J., Blaney, D., Blank, J., Blau, H., Bleacher, L., Boehm, E., Botta, O., Böttcher, S., Boucher, T., Bower, H., Boyd, N., Boynton, B., Breves, E., Bridges, J., Bridges, N., Brinckerhoff, W., Brinza, D., Brunet, C., Brunner, A., Brunner, W., Buch, A., Bullock, M., Burmeister, S., Cabane, M., Calef, F., Cameron, J., Campbell, J. Iain, Cantor, B., Caplinger, M., Caride Rodríguez, J., Carmosino, M., Carrasco Blázquez, I., Charpentier, A., Choi, D., Clark, B., Clegg, S., Cleghorn, T., Cloutis, E., Cody, G., Coll, P., Conrad, P., Coscia, D., Cousin, A., Cremers, D., Cros, A., Cucinotta, F., d'Uston, C., Davis, S., Day, M. Kenzie, De La Torre Juarez, M., DeFlores, L., DeLapp, D., DeMarines, J., Dietrich, W., Dingler, R., Donny, C., Drake, D., Dromart, G., Dupont, A., Duston, B., Dworkin, J., Dyar, M.D., Edgar, L., Edwards, C., Edwards, L., Ehresmann, B., Eigenbrode, J., Elliott, B., Elliott, H., Ewing, R., Fabre, C., Fairén, A., Farley, K., Fassett, C., Favot, L., Fay, D., Fedosov, F., Feldman, J., Feldman, S., Fisk, M., Fitzgibbon, M., Flesch, G., Floyd, M., Flückiger, L., Forni, O., Fraeman, A., Francis, R., François, P., Franz, H., Freissinet, C., French, K.L., Frydenvang, J., Gaboriaud, A., Gailhanou, M., Garvin, J., Gasnault, O., Geffroy, C., Gellert, R., Genzer, M., Glavin, D., Godber, A., Goesmann, F., Goetz, W., Golovin, D., Gómez Gómez, F., Gómez-Elvira, J., Gondet, B., Gordon, S., Gorevan, S., Grant, J., Griffes, J., Grinspoon, D., Guillemot, P., Guo, J., Guzewich, S., Haberle, R., Halleaux, D., Hallet, B., Hamilton, V., Hardgrove, C., Harker, D., Harpold, D., Harri, A.-M., Harshman, K., Hassler, D., Haukka, H., Hayes, A., Herkenhoff, K., Herrera, P., Hettrich, S., Heydari, E., Hipkin, V., Hoehler, T., Hollingsworth, J., Hudgins, J., Huntress, W., Hviid, S., Iagnemma, K., Indyk, S., Israël, G., Jackson, R., Jacob, S., Jakosky, B., Jensen, E., Jensen, J.K., Johnson, J., Johnson, M., Johnstone, S., Jones, A., Jones, J., Joseph, J., Jun, I., Kah, L., Kahanpää, H., Kahre, M., Karpushkina, N., Kasprzak, W., Kauhanen, J., Keely, L., Kemppinen, O., Keymeulen, D., Kim, M.-H., Kinch, K., King, P., Kirkland, L., Kocurek, G., Koefoed, A., Köhler, J., Kortmann, O., Kozyrev, A., Krezoski, J., Krysak, D., Kuzmin, R., Lacour, J.L., Lafaille, V., Langevin, Y., Lanza, N., Lasue, J., Le Mouélic, S., Lee, E.M., Lee, Q.-M., Lees, D., Lefavor, M., Lemmon, M., Malvitte, A.L., Leshin, L., Léveillé, R., Lewin-Carpintier, É., Lewis, K., Li, S., Lipkaman, L., Little, C., Litvak, M., Lorigny, E., Lugmair, G., Lundberg, A., Lyness, E., Madsen, M., Mahaffy, P., Maki, J., Malakhov, A., Malespin, C., Malin, M., Mangold, N., Manhes, G., Manning, H., Marchand, G., Marín Jiménez, M., Martín García, C., Martin, D., Martin, M., Martínez-Frías, J., Martín-Soler, J., Martín-Torres, F.J., Mauchien, P., McAdam, A., McCartney, E., McConnochie, T., McCullough, E., McEwan, I., McKay, C., McNair, S., Melikechi, N., Meslin, P.-Y., Meyer, M., Mezzacappa, A., Miller, H., Miller, K., Minitti, M., Mischna, M., Mitrofanov, I., Moersch, J., Mokrousov, M., Molina Jurado, A., Moores, J., Mora-Sotomayor, L., Mueller-Mellin, R., Muller, J.-P., Muñoz Caro, G., Nachon, M., Navarro López, S., Navarro-González, R., Nealson, K., Nefian, A., Nelson, T., Newcombe, M., Newman, C., Nikiforov, S., Niles, P., Nixon, B., Noe Dobrea, E., Nolan, T., Oehler, D., Ollila, A., Olson, T., Owen, T., De Pablo Hernández, M.Á., Paillet, A., Pallier, E., Palucis, M., Parker, T., Parot, Y., Patel, K., Paton, M., Paulsen, G., Pavlov, A., Pavri, B., Peinado-González, V., Pepin, R., Peret, L., Perez, R., Perrett, G., Peterson, J., Pilorget, C., Pinet, P., Pla-García, J., Plante, I., Poitrasson, F., Polkko, J., Popa, R., Posiolova, L., Posner, A., Pradler, I., Prats, B., Prokhorov, V., Purdy, S.W., Raaen, E., Radziemski, L., Rafkin, S., Ramos, M., Raulin, F., Ravine, M., Reitz, G., Rennó, N., Richardson, M., Robert, F., Robertson, K., Rodriguez Manfredi, J.A., Romeral-Planelló, J.J., Rowland, S., Rubin, D., Saccoccio, M., Salamon, A., Sandoval, J., Sanin, A., Sans Fuentes, S.A., Saper, L., Sautter, V., Savijärvi, H., Schieber, J., Schmidt, M., Schmidt, W., Scholes, D. Dan, Schoppers, M., Schröder, S., Schwenzer, S., Sebastian Martinez, E., Sengstacken, A., Shterts, R., Siebach, K., Siili, T., Simmonds, J., Sirven, J.-B., Slavney, S., Sletten, R., Smith, M., Sobrón Sánchez, P., Spray, J., Squyres, S., Stalport, F., Steele, A., Stein, T., Stern, J., Stewart, N., Stipp, S.L.S., Stoiber, K., Sucharski, B., Sullivan, R., Summons, R., Sun, V., Supulver, K., Sutter, B., Szopa, C., Tan, F., Tate, C., Teinturier, S., Ten Kate, I., Thomas, P., Thompson, L., Tokar, R., Toplis, M., Torres Redondo, J., Trainer, M., Tretyakov, V., Urqui-O'Callaghan, R., Van Beek, J., Van Beek, T., VanBommel, S., Varenikov, A., Vasavada, A., Vasconcelos, P., Vicenzi, E., Vostrukhin, A., Voytek, M., Wadhwa, M., Ward, J., Webster, C., Weigle, E., Wellington, D., Westall, F., Wiens, R.C., Wilhelm, M.B., Williams, A., Williams, R., Williams, R.B. Mouser, Wilson, M., Wimmer-Schweingruber, R., Wolff, M., Wong, M., Wray, J., Wu, M., Yana, C., Yingst, A., Zeitlin, C., Zimdar, R., Zorzano Mier, M.-P., 2014. Mineralogy of a mudstone at Yellowknife Bay, Gale crater, Mars. Science 343, 1243480. https://doi.org/10.1126/science.1243480.

Viennet, J.-C., Bernard, S., Le Guillou, C., Jacquemot, P., Balan, E., Delbes, L., Rigaud, B., Georgelin, T., Jaber, M., 2019. Experimental clues for detecting biosignatures on Mars. Geochem. Perspect. Lett. 28–33. https://doi.org/10.7185/geochemlet.1931.

Viennet, J.-C., Bernard, S., Le Guillou, C., Jacquemot, P., Delbes, L., Balan, E., Jaber, M., 2020. Influence of the nature of the gas phase on the degradation of RNA during fossilization processes. Appl. Clay Sci. 191, 105616. https://doi.org/10.1016/j.clay.2020.105616.

Viennet, J.-C., Roskosz, M., Nakamura, T., Beck, P., Baptiste, B., Lavina, B., Alp, E.E., Hu, M.Y., Zhao, J., Gounelle, M., Brunetto, R., Yurimoto, H., Noguchi, T., Okazaki, R., Yabuta, H., Naraoka, H., Sakamoto, K., Tachibana, S., Yada, T., Nishimura, M., Nakato, A., Miyazaki, A., Yogata, K., Abe, M., Okada, T., Usui, T., Yoshikawa, M., Saiki, T., Tanaka, S., Terui, F., Nakazawa, S., Watanabe, S.-I., Tsuda, Y., 2023. Interaction between clay minerals and organics in asteroid Ryugu. Geochem. Persp. Let. 25, 8–12. https://doi.org/10.7185/geochemlet.2307.

Vinogradoff, V., Le Guillou, C., Bernard, S., Viennet, J.C., Jaber, M., Remusat, L., 2020a. Influence of phyllosilicates on the hydrothermal alteration of organic matter in asteroids: experimental perspectives. Geochim. Cosmochim. Acta 269, 150–166. https://doi.org/10.1016/j.gca.2019.10.029.

Vinogradoff, V., Remusat, L., McLain, H.L., Aponte, J.C., Bernard, S., Danger, G., Dworkin, J.P., Elsila, J.E., Jaber, M., 2020b. Impact of phyllosilicates on amino acid formation under Asteroidal conditions. ACS Earth Space Chem. 4, 1398–1407. https://doi.org/10.1021/acsearthspacechem.0c00137.

Wang, J., Morin, C., Li, L., Hitchcock, A.P., Scholl, A., Doran, A., 2009. Radiation damage in soft X-ray microscopy. J. Electron Spectrosc. Relat. Phenom. 170, 25–36. https://doi.org/10.1016/j.elspec.2008.01.002.

Yuan, P., Liu, H., Liu, D., Tan, D., Yan, W., He, H., 2013. Role of the interlayer space of montmorillonite in hydrocarbon generation: an experimental study based on high temperature–pressure pyrolysis. Appl. Clay Sci. 75–76, 82–91. https://doi.org/10.1016/j.clay.2013.03.007.